Available online at www.sciencedirect.com
SCIENCE DIRECT®
Journal of Sound and Vibration 281 (2005) 1037–1055
JOURNAL OF SOUND AND VIBRATION
www.elsevier.com/locate/jsvi

Implementation of an active vibration controller for gear-set shaft using μ-analysis

Jian-Da Wu*, Jia-Hong Lin

Department of Mechanical and Automation Engineering, Da-Yeh University, 112 Shan-Jiau Road, Da-Tsuen, Changhua 515, Taiwan, ROC

Received 28 May 2003; received in revised form 22 December 2003; accepted 12 February 2004
Available online 29 September 2004

Abstract

A digital signal processor (DSP) implementation of an active vibration controller for reducing periodic vibration in a gear-set shaft is described in this paper. The proposed control algorithms are developed using μ-analysis to obtain robust stability and robust performance in experimental investigation. In experimental work, three different active vibration control algorithms are used, and their characteristics and performances are compared in various experiments. Apart from the traditional adaptive filter and the robust feedback control system, a hybrid controller combining an adaptive controller with a filtered-x least mean squares algorithm and a state feedback theory with a μ-analysis to obtain robust performance and fast convergence is proposed. The control plants are identified by the frequency-domain technique and implemented on a DSP platform. Experiments are carried out to evaluate the attenuation performance and characteristic of three control structures in gear-set shaft vibration. The experimental results indicated that all the three controllers are effective in reducing the gear-set shaft vibration and the hybrid controller demonstrated the best performance in experimental investigation.

*Corresponding author. Present address: Institute of Vehicle and Rail Technology, National Changhua University of Education, 1 Jin-De Road, Changhua 500, Taiwan, ROC. Tel.: +886-931-652880; fax: +886-4-22933183.
E-mail address: jdwu@cc.ncue.edu.tw (J.-D. Wu).

0022-460X/$ - see front matter © 2004 Elsevier Ltd. All rights reserved.
doi:10.1016/j.jsv.2004.02.004

1. Introduction

Owing to the progress in digital signal processing (DSP) algorithms and hardware, active control is beginning to make breakthroughs in many practical applications. In particular, active vibration control (AVC) with modern digital control algorithm and technology has been extensively investigated both theoretically and experimentally [1–3]. In the last two decades, AVC technique has advanced rapidly and has become a promising alternative to conventional passive control, thanks to improvements in DSP technology. The DSP has tended to concentrate on real-time implementation at fast sample rates [4–6]. Many of the sophisticated control algorithms and techniques have also been implemented on DSP platforms for practical applications. In particular, AVC with synthesis vibration source has been extensively investigated [7].

In active-control structures, adaptive control has become the most widely used method to reduce noise and vibration when a reference signal is available. For an adaptive control, the filtered-x least mean squares (FXLMS) algorithm is the most well known, having been applied extensively in many applications such as adaptive active noise cancellation in a duct [8] and active vibration control in a rotor [9]. In 1999, Rebbechi et al. developed an adaptive AVC system to reduce gearbox shaft vibration [10]. Other applications such as in helicopter vibration and rotor vibration control were also developed [11–14]. To date, adaptive control in AVC application is one of the effective methods; however, when practically applying the FXLMS algorithm, the convergence speed causes limitations because the adaptive algorithm learning process fails to respond fast enough to the changing operation conditions. Meanwhile, in a practical application, the reference signal is not always obtained. In this case, a feedback control structure could be used to improve the control performance [15]. For feedback structures, the Linear Quadratic Gaussian (LQG) control theory is a well-known control method, which can supply a simple and effective control method to solve optimal least-squares problems [16,17]. However, problems of stability will arise and control performance will also fall because it does not consider system uncertainties. Therefore, H_∞ control algorithm was proposed to replace LQG in practical design in 1981, which considers the effect of uncertainties in a control system [18]. The objective of H_∞ control is to minimize the maximum amplitude magnification factor of the primary system and to solve robustness in the control system. It means that perturbation between the real plant and the nominal plant should be considered in designing an AVC controller. The common causes of plant uncertainties are error of measurement, error of modeling and error of computation in physical conditions. Actually, in a control system, plant uncertainty is one of the major factors that can affect nominal performance, robust stability and robust performance. For example, in a rotation system, plant uncertainty may be caused by shaft speed change.

Recently, μ-synthesis has been considered as an effective approach because it can increase robust performance in a control system [19,20]. In this study, a μ-synthesis method is used for improving robust performance in a gear-set shaft vibration control system. Meanwhile, a hybrid control algorithm consisting of a combination of an adaptive control with an FXLMS algorithm and a feedback structure with a μ-synthesis theory to obtain fast convergence and robust performance is also proposed. In controller design, the μ-analysis robust control is used to overcome plant structure uncertainties. The proposed AVC system is implemented on a TMS320C32 floating-point DSP platform to reduce the gear-set shaft vibration. Experimental investigations are implemented to compare the attenuation performance of an adaptive controller,

a feedback controller and the proposed hybrid controller. The control algorithm of three control structures and experimental description are described in the following sections.

2. Control structures of AVC system

2.1. Adaptive AVC system

The multi-input multi-output (MIMO) FXLMS algorithm with synthetic reference is utilized in the control structure [21]. In this study, control structure is a $1 \times 2 \times 2$ system (one reference sensor signal; two error sensor signals; two secondary sources), as shown in Fig. 1. The reference input signal of the AVC system, $x(k)$, is generated from a signal generator with an optical fiber sensor signal input. The $e(k)$ is an error signal, which is obtained from an accelerometer, and the $y(k)$ is a control signal to shakers. The block diagram of a $1 \times 2 \times 2$ AVC system using the FXLMS control algorithm is shown in Fig. 2, where $x(k)$ is the reference input signal; the vibration signal $m(k)$ is generated from a motor; $P_1(z)$ and $P_2(z)$ are the primary paths from the vibration source to the two error sensors; the error signals $e_1(k)$ and $e_2(k)$ are the residual vibrations of the shaft; the output signals $y_1(k)$ and $y_2(k)$ are generated from the adaptive filters $W_1(z)$ and $W_2(z)$; $S_{11}(z)$ and $S_{21}(z)$ are the secondary paths from $y_1(k)$ to two error sensors; $S_{12}(z)$ and $S_{22}(z)$ are the secondary paths from $y_2(k)$ to two error sensors. The transfer function $\hat{S}_{mn}(z)$ is the estimation of $S_{mn}(z)$ for $m = 1, 2$ and $n = 1, 2$. The weight vector update is as follows:

$$w_n(k+1) = w_n(k) + \mu \sum_{m=1}^{2} x'_{mn}(k) e_m(k), \quad n = 1, 2, \tag{1}$$

where μ is the convergence factor.

In Eq. (1), μ is the step size that will affect the stability and convergence rate of a system. It is inversely proportional to the convergence time. Care should be taken to decide the step size value μ and the length of the least mean squares order. In general, a large μ guarantees the tracking

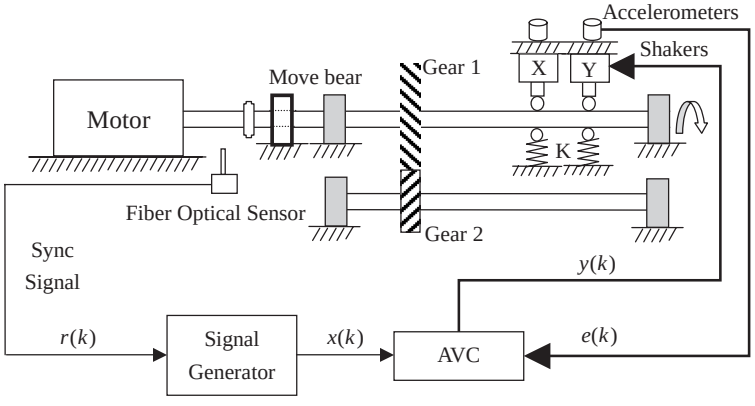

Fig. 1. Adaptive AVC system in a gear-set system.

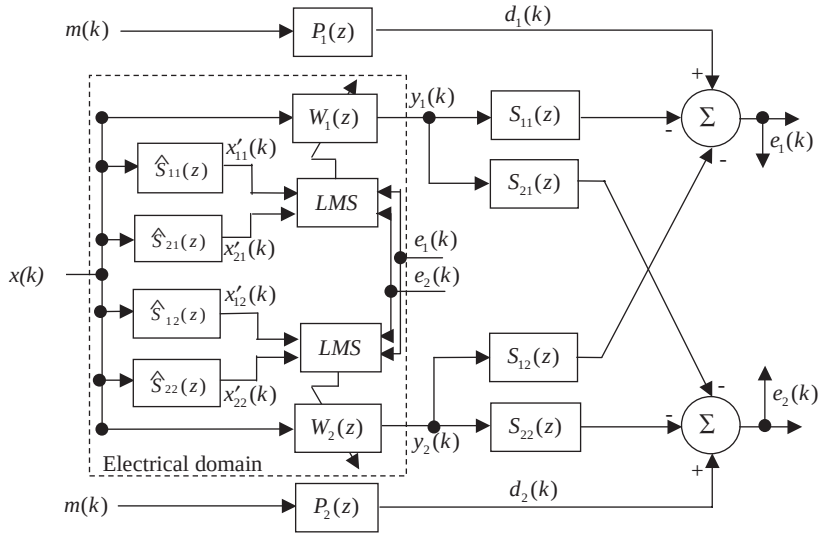

Fig. 2. Block diagram of a $1 \times 2 \times 2$ AVC with FXLMS algorithm.

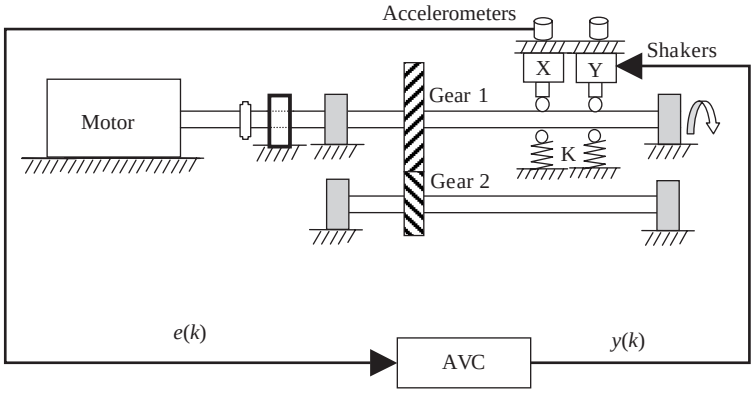

Fig. 3. Feedback AVC system in a gear-set system.

capability of the algorithm; however, this capability is reduced when the mean-square error (MSE) is excessively large. In contrast, a small μ will affect the tracking capability and the convergence speed. Therefore, the selection of the optimal convergence factor in an adaptive control structure is important.

2.2. μ-analysis AVC system

The generalized control framework of feedback control in a gear-set system is shown in Fig. 3 [22]. It contains the vibration signal $e(k)$, which is measured using two accelerometers, and the output signal $y(k)$. The general problem of H_∞ controller design is formed in a configuration as

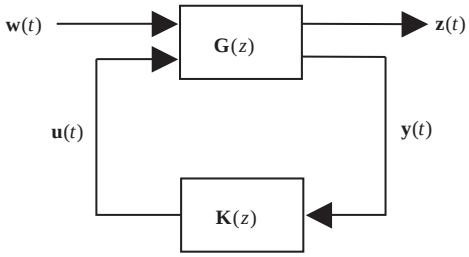

Fig. 4. Generalized control framework in robust control theory.

the augmented plant $\mathbf{G}(z)$ shown in Fig. 4 is combined with a weighting function and practical plant. In the structure, $\mathbf{K}(z)$ is the controller, $\mathbf{w}(t)$ is the vector signal including noise, disturbances, and reference signal. $\mathbf{u}(t)$ is the control signal, $\mathbf{z}(t)$ is the vector signal including all controller signals and tracking errors, and $\mathbf{y}(t)$ is the measured output signal. The system model can be expressed by

$$\begin{bmatrix}\mathbf{z}(z)\\ \mathbf{y}(z)\end{bmatrix} = \mathbf{G}(z)\begin{bmatrix}\mathbf{w}(z)\\ \mathbf{u}(z)\end{bmatrix} = \begin{bmatrix}\mathbf{G}_{11}(z) & \mathbf{G}_{12}(z)\\ \mathbf{G}_{21}(z) & \mathbf{G}_{22}(z)\end{bmatrix}\begin{bmatrix}\mathbf{w}(z)\\ \mathbf{u}(z)\end{bmatrix}, \tag{2}$$

$$\mathbf{U}(z) = \mathbf{K}(z)\mathbf{Y}(z),$$

where the sub-matrices $\mathbf{G}_{ij}(z)$ are the compatible partition of the augmented plant $\mathbf{G}(z)$; signal variables are capitalized to represent symbols in the S-domain.

The H_∞ control system is used to find a stable controller $\mathbf{K}(z)$ that minimizes the infinity norm of the transfer function from $\mathbf{w}(z)$ to $\mathbf{z}(z)$ denoted by $\|\mathbf{T}_{zw}(z)\|_\infty$, where

$$\|\mathbf{T}_{zw}(z)\|_\infty = \sup_{\substack{\omega\neq 0\\(-\infty,\infty)}} |\mathbf{T}_{zw}(\mathrm{j}\omega)|. \tag{3}$$

$\mathbf{T}_{zw}(z)$ can be expressed by lower linear fraction transformation (LFT) as

$$\mathbf{T}_{zw}(\mathrm{z}) = F_1(\mathbf{P},\mathbf{K}) = \mathbf{G}_{11}(z) + \mathbf{G}_{12}(z)\mathbf{K}(z)[\mathbf{I} - \boldsymbol{G}_{22}(z)\mathbf{K}(z)]^{-1}\mathbf{G}_{21}(z). \tag{4}$$

However, finding an optimal H_∞ controller is often complicated. In practice, we try to find an admissible controller $\mathbf{K}(z)$ for the $\mathbf{T}_{zw}(z)$ system, that easily satisfies the infinity norm and that will be called *suboptimal controller*. The sub-optimal controller $\mathbf{K}(z)$ is given by $\gamma > 0$; stabilizing controllers as

$$\|\mathbf{T}_{zw}(z)\|_\infty < \gamma. \tag{5}$$

In the proposed study, an uncertainty model is included in H_∞ control structure. Therefore, the μ-analysis is introduced to obtain better robust performance. The μ-analysis control structure can be cast into a generalized control framework, as depicted in Fig. 5. The framework contains a controller $\mathbf{K}(z)$, an augmented plant $\mathbf{G}(z)$ and an uncertainty $\mathbf{\Delta}(z)$. The input signal $\mathbf{d}(t)$ and output signal $\mathbf{v}(t)$ of uncertainty $\mathbf{\Delta}(z)$ correspond to model uncertainties or perturbations, while $\mathbf{w}(t)$, $\mathbf{u}(t)$, $\mathbf{z}(t)$ and $\mathbf{y}(t)$ have been defined as in Fig. 4. The closed-loop transfer function $\mathbf{M}(\mathbf{G},\mathbf{K})$ is illustrated

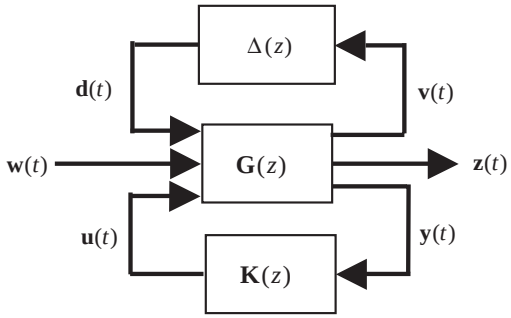

Fig. 5. Generalized framework in μ-analysis control theory.

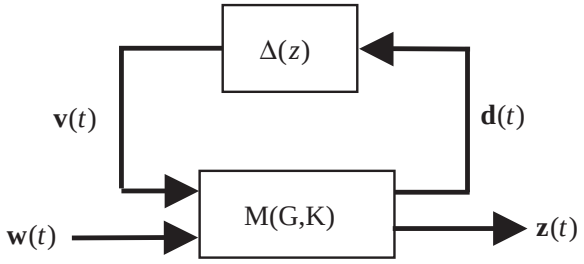

Fig. 6. Linear fractional transformation with an uncertainty model.

in Fig. 6. The transfer function from $\mathbf{w}(t)$ to $\mathbf{z}(t)$ is represented by way of linear fractional transformation (LFT),

$$z = F_u(\mathbf{M}, \mathbf{\Delta})\mathbf{w} = [\mathbf{M}_{22}(z) + \mathbf{M}_{21}(z)\mathbf{\Delta}(z)(\mathbf{I} - \mathbf{M}_{11}(z)\mathbf{\Delta}(z))^{-1}\mathbf{M}_{12}(z)]\mathbf{w},$$

where

$$\begin{bmatrix} \mathbf{d}(t) \\ \mathbf{z}(t) \end{bmatrix} = \mathbf{M}\begin{bmatrix} \mathbf{v}(t) \\ \mathbf{w}(t) \end{bmatrix} = \begin{bmatrix} \mathbf{M}_{11} & \mathbf{M}_{12} \\ \mathbf{M}_{21} & \mathbf{M}_{22} \end{bmatrix}\begin{bmatrix} \mathbf{v}(t) \\ \mathbf{w}(t) \end{bmatrix}. \tag{6}$$

The uncertainty model $\mathbf{\Delta}(z)$ is assumed to belong to the set

$$\mathbf{\Delta} = \left\{\mathrm{diag}(\delta_1\mathbf{I}_{s_1}, \ldots, \delta_k\mathbf{I}_{s_k}, \mathbf{\Delta}_1, \ldots, \mathbf{\Delta}_r) : \delta_i \in C,\ \ \mathbf{\Delta}_j \in C^{m_j \times m_i}\right\}, \tag{7}$$

For all perturbations $\Delta \in \mathbf{\Delta}$ satisfying $\max \bar{\sigma}(\Delta) \leqslant 1$, it can be written as

$$B_\Delta := \{\Delta \in \mathbf{\Delta} : \bar{\sigma}(\Delta) \leqslant 1\}, \tag{8}$$

where $\delta_i\mathbf{I}_{sk}$ is the repeated scalar blocks uncertainty, $\mathbf{\Delta}_j$ is the full blocks uncertainty, and $\bar{\sigma}$ denotes the maximum singular value. Two non-negative integers (k and r) represent the number of repeated scalar blocks and the number of full blocks, respectively. The dimension of the ith repeated scalar blocks is $s_i \times s_i$, while the jth full blocks is $m_j \times m_i$ [23].

In μ-analysis, the structured singular value μ is a generalization of a singular value. It is used to analyze robust stability and robust performance in a system with structured uncertainty. The structured singular value μ of a system $\mathbf{M}$ is defined as

$$\mu_{\Delta}(\mathbf{M}) := (\min\{\bar{\sigma}(\Delta): \Delta \in \mathbf{\Delta}, \det(\mathbf{I} - \mathbf{M}\mathbf{\Delta}) = 0\})^{-1}, \tag{9}$$

which is a measurement of the smallest uncertainty that may destabilize the closed-loop system. In Fig. 6, uncertainty affects stability and performance of a system and is indicated as follows:

(A) *Nominal performance* is by setting model uncertainty $\mathbf{\Delta}(z)$ in the problem formulation to zero; it is just a norm test on $\left\|\mathbf{T}_{zw}(z)\right\|_{\infty} < 1$ or $\|\mathbf{M}_{22}\|_{\infty} < 1$ [24].
(B) *Robust stability* has to think about structure uncertainty in Fig. 6. That must suffice for $\|\mathbf{T}_{vd}\|_{\mu} < 1$ or $\|\mathbf{M}_{11}\|_{\mu} < 1$. In this part, $\|\bullet\|_{\mu}$ is not norm; it is a structured singular value test.
(C) *Robust performance* is to suffice for (A) and (B) and reach $\left\|\mathbf{M}(\mathbf{G}, \mathbf{K})\right\|_{\mu} < 1$. This part implies that performance objective described in terms of infinity norm test, robust performance of any linear, time-invariant system in the presence of structured uncertainty can be written as a structured singular value test.

2.3. The hybrid AVC structure

In this section, an adaptive hybrid active vibration controller for gear-set shaft vibration attenuation is proposed. The hybrid control structure is shown in Fig. 7, the reference input signal $x(k)$ is obtained from an optical fiber sensor; the error signals $e(k)$ are measured from two accelerometers; $y(k)$ are the control signals to shakers; T_{FF} is an adaptive controller with FXLMS algorithm, and T_{FB} is a feedback μ-analysis controller. The proposed system differs from

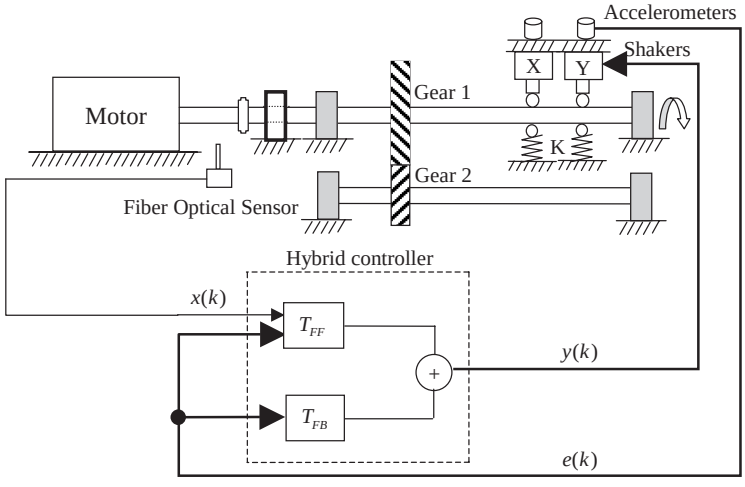

Fig. 7. Hybrid AVC system in a gear-set system.

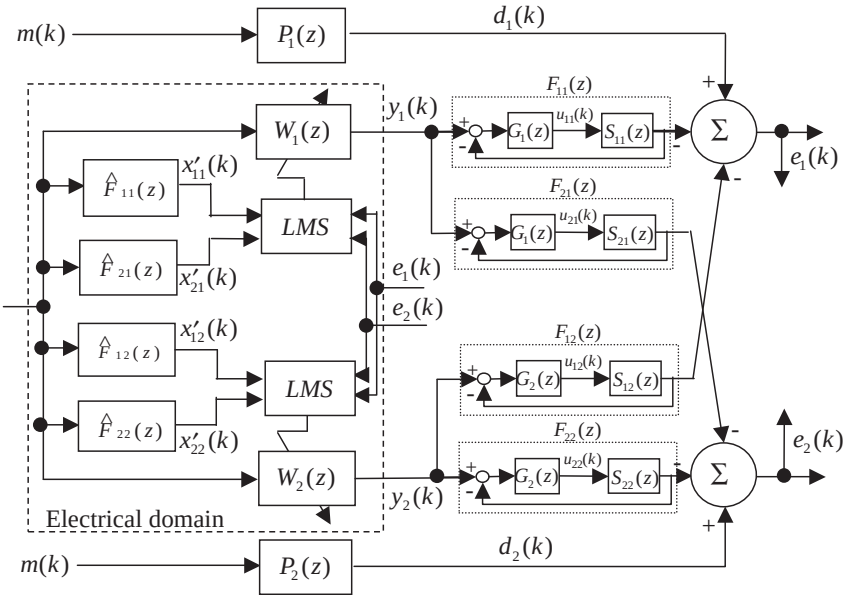

Fig. 8. Block diagram of hybrid control system.

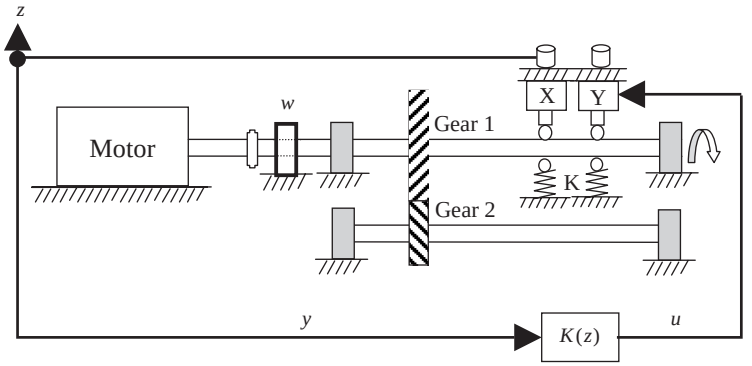

Fig. 9. AVC system of a gear-set system in feedback structure.

the traditional adaptive algorithm in that it uses an internal model control as shown in Fig. 8, where $F_{mn}(z)$ is the feedback controller essential point (FCEP) and is defined by $F_{mn}(z) = [1 + G_n(z)S_{mn}(z)]^{-1}G_n(z)S_{mn}(z)$. $G_n(z)$ is an H_∞ μ-analysis controller with two plant functions and two weighting functions, $u_{mn}(k)$ are the control signals, and $S_{mn}(z)$ are the secondary paths in the FCEP. In the electrical domain of Fig. 8, the transfer functions $\hat{F}_{mn}(z)$ are estimations of $F_{mn}(z)$ that stabilize the closed-loop system and that include a μ-analysis feedback controller and secondary path transfer function. The model design of $F_{mn}(z)$ is necessary to overcome plant uncertainties to obtain fast convergence and robust performance.

In this hybrid structure, the FXLMS algorithm is compensated by an H_∞ feedback controller T_{FB} in closed loop. In order to obtain both fast convergence and stability, step size μ is an

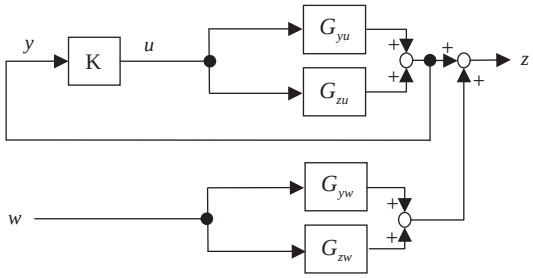

Fig. 10. Equivalent block diagram of a gear-set system.

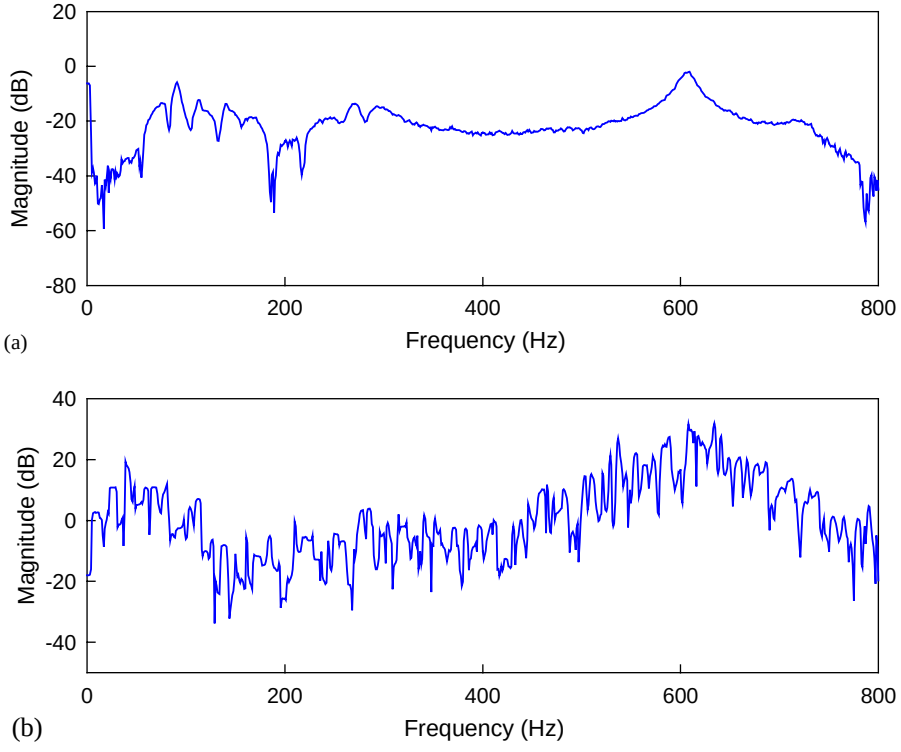

Fig. 11. Frequency responses of the real plants measured within 0–800 Hz. (a) Frequency response of $G_{zu}(z)$ and $G_{yu}(z)$; (b) frequency response of $G_{zw}(z)$ and $G_{yw}(z)$.

approximate upper bound in the FXLMS algorithm as follows:

$$0<\mu<\frac{2}{P_r(L+2D+2)}, \tag{10}$$

where $P_r = E[x^2(k)]$ is the reference signal power function, L is the order of filter $W_n(z)$, and D is the small delay of the secondary path [25]. Hence, a small size μ can be used as hybrid controller to obtain fast convergent and tracking performance.

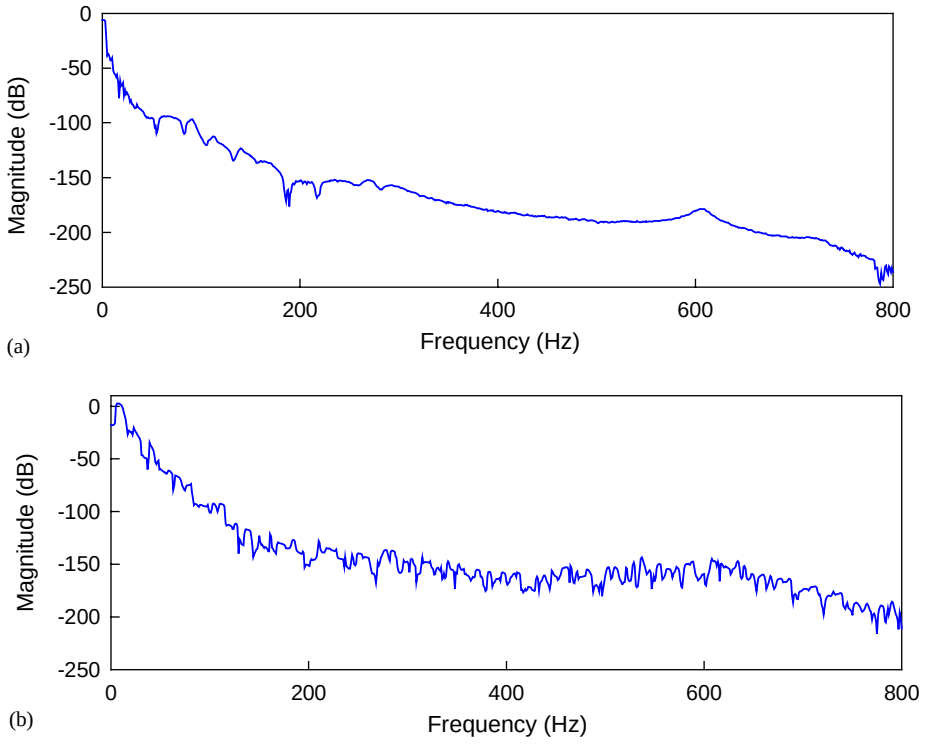

Fig. 12. Frequency responses of the nominal plants measured by low pass. (a) Frequency response of $G_{zu}(z)$ and $G_{yu}(z)$; (b) frequency response of $G_{zw}(z)$ and $G_{yw}(z)$.

3. μ-analysis of a gear-set system

The structure of the proposed gear-set system in feedback structure is shown in Fig. 9. In a robust control structure, the augmented plant relation is expressed as

$$\begin{bmatrix} z(t) \\ y(t) \end{bmatrix} = \begin{bmatrix} G_{zw}(z)G_{zu}(z) \\ G_{yw}(z)G_{yu}(z) \end{bmatrix} \begin{bmatrix} w(t) \\ u(t) \end{bmatrix}, \tag{11}$$

where $G_{zw}(z)$, $G_{zu}(z)$, $G_{yw}(z)$ and $G_{yu}(z)$ are the compatible partition of augmented plant **G**; they are shown in Fig. 10. An uncertainty of frequency domain multiplicative type is used in robust μ-analysis for a gear-set AVC system. The problem can be indicated as

$$\Delta(z) = \frac{P_{\mathrm{ph}}(z)}{P_{\mathrm{no}}(z)} - 1, \tag{12}$$

where $P_{\mathrm{ph}}(z)$ is the physical plant, $P_{\mathrm{no}}(z)$ is the nominal plant and $\Delta(z)$ represents the multiplicative uncertainty [26]. In the present case, the frequency response function is measured by the signal analyzer. The four frequency response functions of partition plants are measured in 0–800 Hz for the physical plants as shown in Fig. 11(a) and (b), whereas the four frequency responses measured in 0–30 Hz are regarded by low pass as the nominal plants as shown in

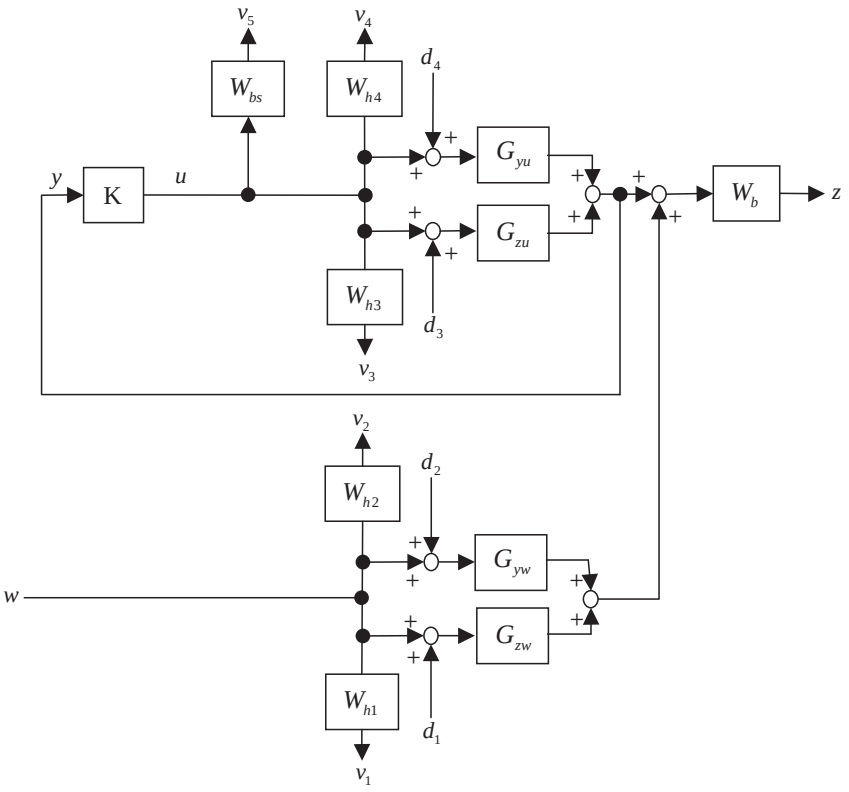

Fig. 13. Interconnected structure which considers uncertainty.

Fig. 12(a) and (b). Fig. 13 illustrates the block diagram of the structure system considering uncertainty. In Fig. 5, the generalized framework in μ-analysis control, the input–output relationwhich includes the multiplicative uncertainty of the augmented plant, is described as follows:

$$\begin{bmatrix} v_1 \\ v_2 \\ v_3 \\ v_4 \\ v_5 \\ z \\ y \end{bmatrix} = \mathbf{G} \begin{bmatrix} d_1 \\ d_2 \\ d_3 \\ d_4 \\ w \\ u \end{bmatrix} = \begin{bmatrix} 0 & 0 & 0 & 0 & W_{h1} & 0 \\ 0 & 0 & 0 & 0 & W_{h2} & 0 \\ 0 & 0 & 0 & 0 & 0 & W_{h3} \\ 0 & 0 & 0 & 0 & 0 & W_{h4} \\ 0 & 0 & 0 & 0 & 0 & W_{\mathrm{bs}} \\ W_b G_{zw} & W_b G_{yw} & W_b G_{zu} & W_b G_{yu} & W_b(G_{yw}+G_{zw}) & W_b(G_{yu}+G_{zu}) \\ 0 & 0 & G_{zu} & G_{yu} & 0 & (G_{yu}+G_{zu}) \end{bmatrix} \begin{bmatrix} d_1 \\ d_2 \\ d_3 \\ d_4 \\ w \\ u \end{bmatrix}. \quad (13)$$

The term W_b is a performance weight function for disturbance rejection in the desired frequency band and W_{bs} is a controller weight function to restrict the controller gain out of controlled frequencies. In the present case, W_b and W_{bs} are chosen as band-pass and band-stop weighting functions. Meanwhile, in the present work, the types of uncertainty blocks must be

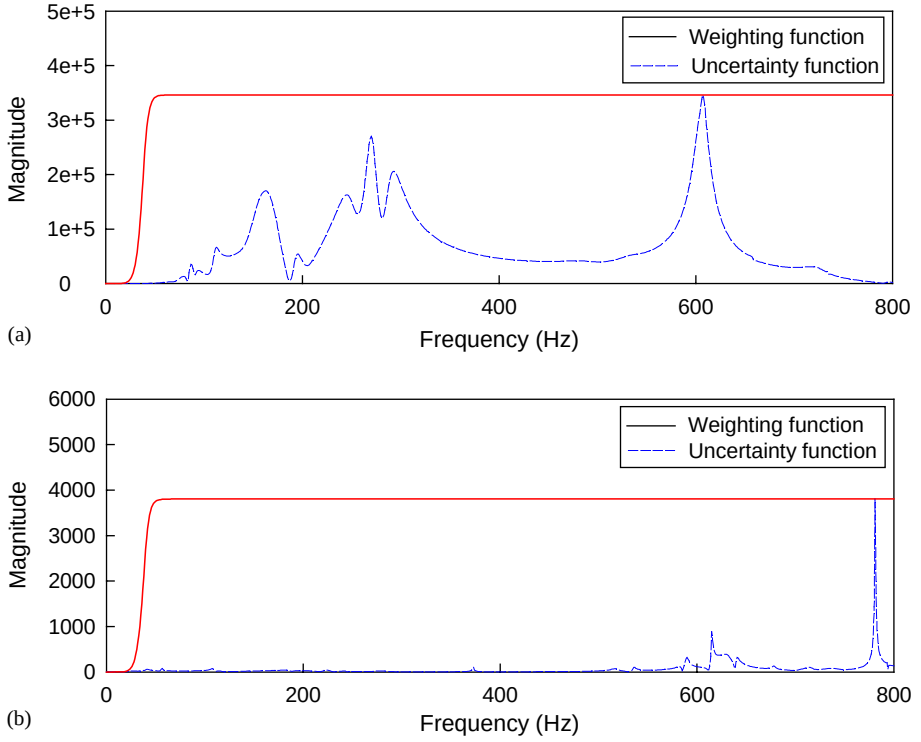

Fig. 14. Uncertainty function and weighing function. (a) Result of calculation for $G_{zu}(z)$ and $G_{yu}(z)$; (b) result of calculation for $G_{zw}(z)$ and $G_{yw}(z)$.

specified. The full complex block is chosen as

$$\Delta := \left\{ \begin{bmatrix} \Delta_1 & 0 \\ 0 & \Delta_2 \end{bmatrix} : \Delta_1 = \begin{bmatrix} \Delta_{11} & 0 & 0 & 0 \\ 0 & \Delta_{12} & 0 & 0 \\ 0 & 0 & \Delta_{13} & 0 \\ 0 & 0 & 0 & \Delta_{14} \end{bmatrix}, \quad \Delta_{11} - \Delta_{14} \in C^{1\times 1}, \Delta_2 \in C^{1\times 2} \right\}, \tag{14}$$

where Δ_1 is the multiplicative uncertainty of Eq. (12) and Δ_2 is a fictitious uncertainty block meant to incorporate the performance objectives on the weighted output sensitivity transfer function into the μ framework. The structure uncertainty of each transfer function is assumed to be bounded by a high-pass weighting function. In Eq. (14), each $W_{h,i}$ is an uncertainty weighting function and must satisfy

$$\left|\Delta(j\omega)\right| \leqslant \left|W_{h,i}(j\omega)\right|, \quad i = 1, 2, 3, 4, \quad \forall\omega. \tag{15}$$

The calculated uncertainty bounded by uncertainty weighting function $W_{h,i}$ is shown in Fig. 14(a) and (b). In addition, uncertainty does not include the control bandwidth (below 30 Hz) due to numerical errors in system identification. Thus, we can estimate the uncertainty of an uncontrolled bandwidth (above 30 Hz) in the system. In this work, the system has robust

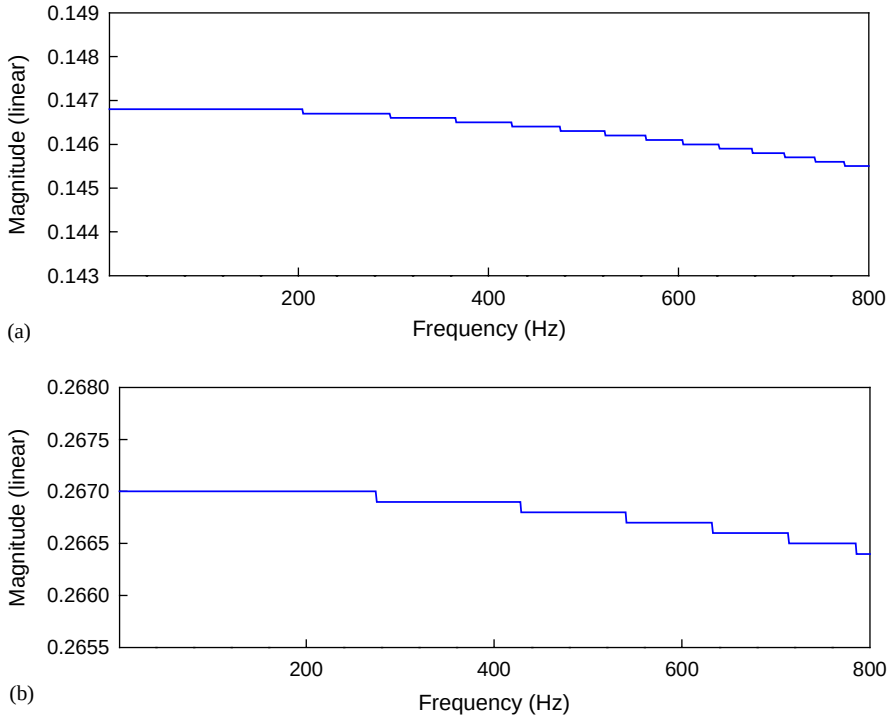

Fig. 15. The μ plots of the system. (a) μ plot of direction X; (b) μ plot of direction Y.

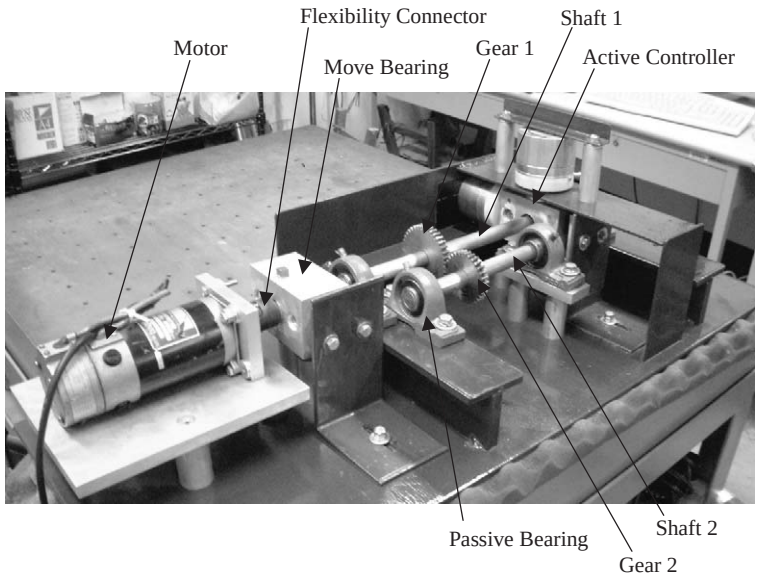

Fig. 16. Photograph of the experimental setup.

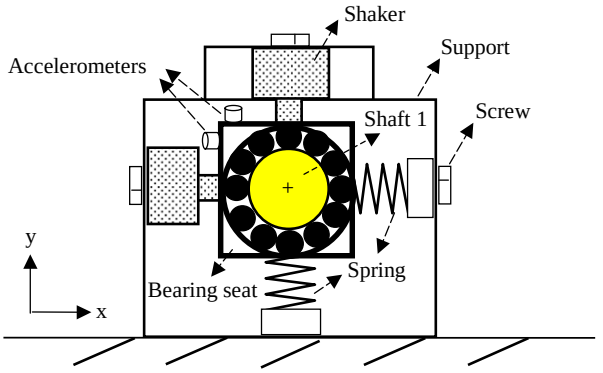

Fig. 17. Internal structure of an active controller.

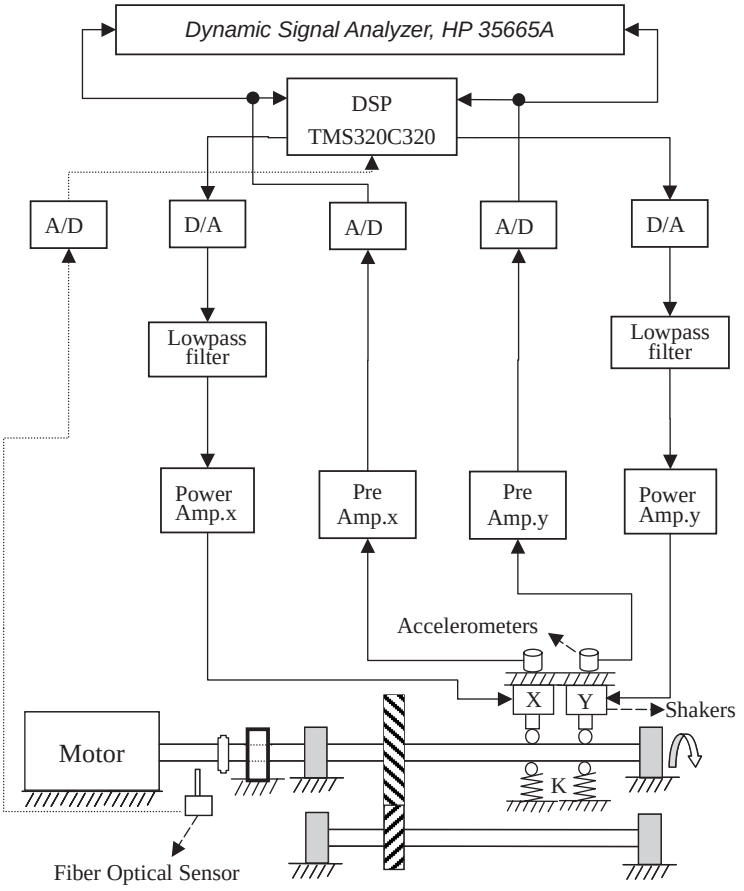

Fig. 18. Experimental setup of AVC system in a gear-set system.

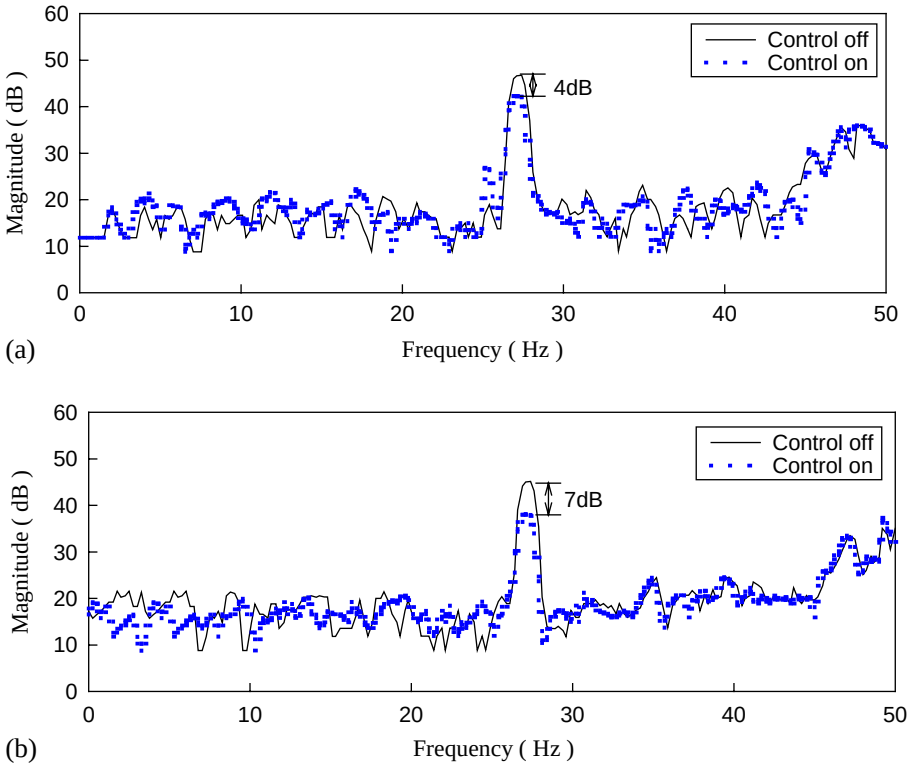

Fig. 19. Experimental results of an adaptive controller. (a) Direction X; (b) direction Y.

performance due to a μ-analysis controller and is considered the effect of structure uncertainty. The bounds for the structured singular values of direction X and Y are shown in Fig. 15(a) and (b) In the μ plot, the values of μ are smaller than 1 within the control bandwidth. Robust performance has been achieved in this system.

4. DSP implementation and experimental investigation

4.1. Experimental arrangement

The photograph of the experimental setup is shown in Fig. 16. The horsepower of DC servo motor is $\frac{1}{2}$, with a maximum rotational speed of 3000 rev/min. The motor can be controlled by using an inverter. The diameter of shafts is 20 mm and the shafts are supported by passive bearings. The tooth number of gear 1 is 40 and of gear 2 is 31. The active controller designed around shaft 1 with two electromagnetic actuators and springs are shown in Fig. 17. The move-bearing structure is a similar active controller. Fig. 18 shows the experimental arrangement components. An optical fiber sensor (LM339) is used to detect the motor rotational speed as a reference signal of the control system. The residual vibration signal is measured by using two

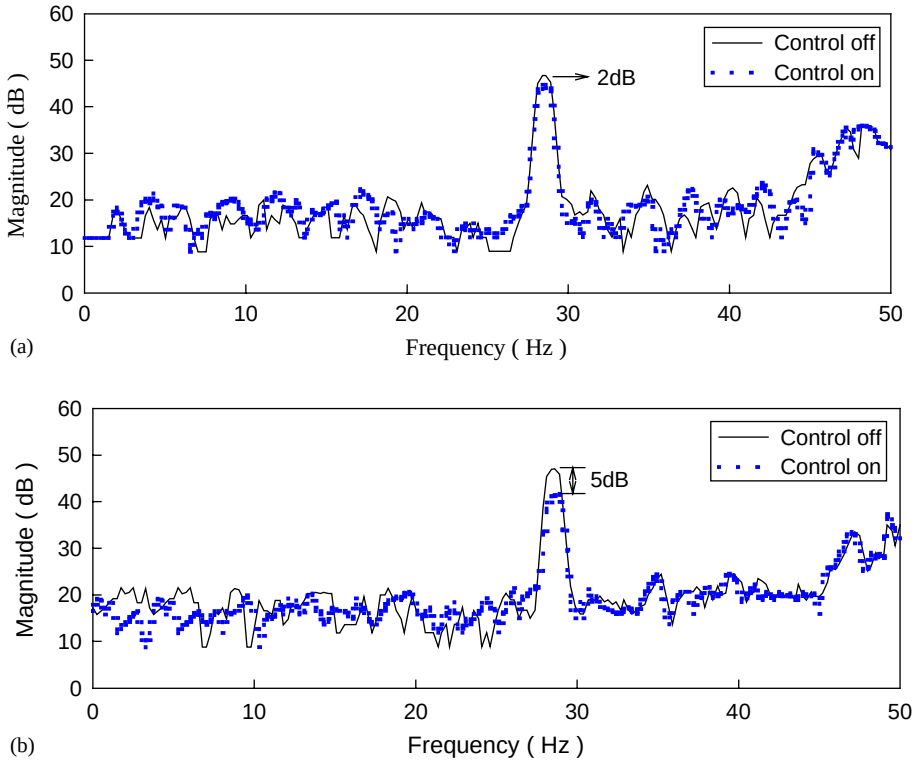

Fig. 20. Experimental results of a μ-analysis controller. (a) Direction X; (b) direction Y.

accelerometers (PCB model 353B15). Two electromagnetic actuators are used to generate the control force to reduce the vibration in the gear-set shaft. The controllers are implemented on a TMS320C32 DSP equipped with two 16-bit analog I/O channels and sampling frequency set at 2048 Hz. Some controller design considerations and control structures verifications in practical implementation are summarized as follow.

4.2. Experimental verification

In the first experimental implementation, an adaptive control with FXLMS algorithm is applied to the test platform. The step size value μ is set at 0.01 and the weight length selected is 30. Frequency-domain identification is used to obtain an adaptive filter. The experimental results in directions X and Y are shown in Fig. 19(a) and (b). Periodic vibration power attenuation values achieved are 4 and 7 dB at 27 Hz (1620 rev/min) of the gear-shaft revolution. In the experiment using feedback μ-analysis algorithm, the gain of W_b is 2 and that of W_{bs} is 1 in controller design. The controller achieves a gamma value of 5.6741 and infinity norm 0.2686. Experimental results of directions X and Y are shown in Fig. 20(a) and (b). Vibration power attenuation is only achieved at about 2 and 5 dB in the directions of X and Y. In the final case of the experiments, a hybrid controller is used to implement the vibration control. The order of the LMS algorithm is 30.

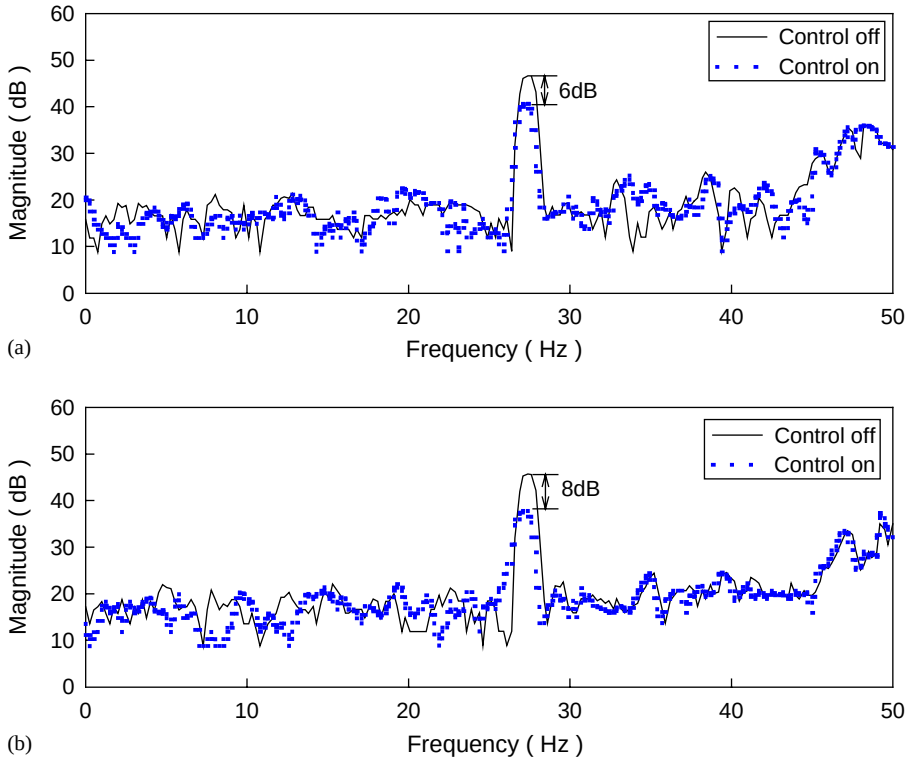

Fig. 21. Experimental results of a hybrid controller. (a) Direction X; (b) direction Y.

Table 1
Experimental results of different control methods

Control method	Adaptive control		μ-analysis control		Hybrid control	
Direction of sensor	X	Y	X	Y	X	Y
Attenuation (dB)	4	7	2	5	6	8
Average attenuation(dB)	5.5		3.5		7	

Table 2
Comparison of three active vibration control systems

Control method	Adaptive control	μ-analysis control	Hybrid control
Uncertainty considered	No	Yes	Yes
Convergence speed	Slow	Fast	Fast
Adaptability	Yes	No	Yes
Robust stability	No	Yes	Yes
System complexity	Simple	Medium	Complex

The step size value μ is set at 0.01. The lower and upper bound parameters of γ are set at $\gamma_{\min} = 1$ and $\gamma_{\max} = 100$, and the step size tolerance value of γ is set at 0.01. Experimental results are shown in Fig. 21(a) and (b). The shaft maximum vibration power attenuation value achieved is about 7 dB at a frequency of 27 Hz.

5. Conclusions

A DSP-based AVC system for reducing the periodic vibration of a gear-set shaft has been investigated. Apart from the adaptive and feedback control system, a hybrid controller combining the adaptive control with the FXLMS algorithm and a feedback structure with robust theory to obtain fast convergence and superior robust performance is proposed. Experimental results show that all the three controllers contribute to reducing gear-set shaft vibration. In practical implementation, the performances of the three different controllers are summarized in Table 1. The adaptive structure, the feedback structure, and the hybrid structure have average attenuation values of about 5.5, 2.5 and 7 dB at gear-set shaft vibration of 27 Hz. In particular, the hybrid controller attenuation performance has the best performance in experimental implementations. However, only narrowband performance has been achieved in the proposed study. The performance of broadband frequency vibration attenuation is poor in implementation investigation. Future research should focus on the development of robust adaptive for broadband vibration attenuation. Comparisons of the crucial parameters in implementation of the gear-set system vibration attenuation are summarized in Table 2. Consequently, the hybrid controller combines the advantages of adaptive with FXLMS algorithm and feedback with μ-analysis theory: better performance, faster convergence, adaptability, robust stability and robust performance of a proposed test platform.

Acknowledgement

The study was supported by the National Science Council of Taiwan, Republic of China, under project number NSC 91-2622-E-212-004.

References

[1] J.D. Wu, M.R. Bai, Effects of directional microphone and transducer in spatially feedforward active noise control system, *Japanese Journal of Applied Physics* 40 (2001) 6133–6137.

[2] L.R. Miller, M. Ahmadian, C.M. Nobles, D.A. Swanson, Modeling and performance of an experimental active vibration isolator, *ASME Journal of Vibration and Acoustics* 117 (1995) 272–278.

[3] M.D. Jenkins, P.A. Nelson, R.J. Pinnington, S.J. Elliott, Active isolation of periodic machinery vibrations, *Journal of Sound and Vibration* 166 (1993) 117–140.

[4] M. Bai, H. Chen, A modified H_2 feedforward active control system for suppressing broadband random and transient noises, *Journal of Sound and Vibration* 198 (1996) 81–94.

[5] D.C. Karnopp, M.J. Crosby, R.A. Harwood, Vibration control using the semiactive force generators, *ASME Journal of Engineering for Industry* 96 (1974) 619–626.

[6] S.J. Elliott, *Signal Processing for Active Control*, Academic Press, New York, 2001.
[7] C.R. Fuller, S.J. Elliott, P.A. Nelson, *Active Control of Vibration*, Harcourt-Brace, San Diego, CA, 1997.
[8] J.D. Wu, M.R. Bai, Application of feed forward adaptive active noise control for reducing blade passing noise in centrifugal fans, *Journal of Sound and Vibration* 239 (2001) 1051–1062.
[9] M.R. Bai, W. Luo, DSP implementation of an active bearing mount for rotors using hybrid control, *ASME Journal of Vibration and Acoustics* 122 (2000) 420–428.
[10] B. Rebbechi, C. Howard, C. Hansen, Active control of gearbox vibration. *Proceedings of the 1999 International Symposium on Active Control of Sound and Vibration,* Florida, USA, 1999, pp. 295–305.
[11] R. Maire, M. Pucher, W. Gembler, H. Schweitzer, Helicopter interior noise reduction by active vibration isolation with smart gearbox struts, *Proceedings of the 1999 International Symposium on Active Control of Sound and Vibration*, Florida, USA, 1999, pp. 189–198.
[12] C.R. Knospe, S.J. Fedigan, R.W. Hope, R.D. Williams, A multitasking DSP implmentation of adaptive magnetic bearing control, *IEEE Transactions on Control Systems Technology* 5 (1997) 230–237.
[13] K.-Y. Lum, V.T. Coppola, D.S. Bernstein, Adaptive autobalancing control for an active magnetic bearing supporting a rotor with unknown mass imbalance, *IEEE Transactions on Control Systems Technology* 4 (1996) 587–597.
[14] K.-Y. Lum, V.T. Coppola, D.S. Bernstein, Adaptive virtual autobalancing for a rigid rotor with unknown mass imbalance supported by magnetic bearing, *ASME Journal of Vibration and Acoustics* 120 (1998) 557–570.
[15] J.M. Macigjowski, *Multivariable Feedback Design*, Addison Wesley, New York, 1990.
[16] J.Y. Lin, H.Y. Sheu, S.C. Chao, LQG/GA design of active noise controllers for a collocated acoustic duct system, *Journal of Sound and Vibration* 228 (1999) 629–650.
[17] F.L. Kim, V.L. Syrmos, *Optimal Control*, Wiley, New York, 1995.
[18] G. Zames, Feedback and optimal sensitivity: model reference transformations, multiplicative seminorms, and approximate inverses, *IEEE Transactions on Automatic Control* 23 (1981) 301–302.
[19] W.-Q. Wang, M. Sznaier, I. Batarseh, J. Bu, Robust controller design for a series resonant converter, *IEEE Transactions on Aerospace and Electronic Systems* 32 (1996) 221–233.
[20] J. Bu, M. Sznaier, W.-Q. Wang, I. Batarseh, Robust controller design for a parallel resonant converter using μ-synthesis, *IEEE Transactions on Aerospace and Electronic Systems* 12 (1997) 837–853.
[21] S.M. Kuo, D.R. Morgan, *Active Noise Control Systems*, Wiley, New York, 1996.
[22] J.C. Doyle, K. Glover, P.P. Khargonehar, B.A. Francis, State-space solution to standard H_2 and H_∞ control problems, *IEEE Transactions on Automatic Control* 34 (1989) 831–847.
[23] G.J. Balas, J.C. Doyle, K. Glover, A. Packard, R. Smith, *μ-Analysis and Synthesis Toolbox: User's Guide*, The Math works Inc., Natick, MA, 1994.
[24] G.J. Balas, J.C. Doyle, A. Packard, Linear, multivariable robust control with a μ perspective, *ASME Journal of Dynamic Systems, Measurement and Control* 115 (1993) 426–438.
[25] G. Long, F. Ling, J.G. Proakis, Corrections to 'The LMS algorithm with delayed coefficient adaptation', *IEEE Transactions on Signal Processing* 40 (1992) 230–232.
[26] J.C. Doyle, B.A. Francis, A.R. Tannenbaum, *Feedback Control Theory*, Maxwell, New York, 1992.